Available online at www.sciencedirect.com
ScienceDirect
International Journal of Heat and Mass Transfer 50 (2007) 1592–1602
International Journal of HEAT and MASS TRANSFER
www.elsevier.com/locate/ijhmt

Scaling investigation of the natural convection boundary layer on an evenly heated plate

S.W. Armfield [a,*], John C. Patterson [b], Wenxian Lin [b]

[a] School of Aerospace, Mechanical and Mechatronic Engineering, The University of Sydney, NSW 2006, Australia
[b] School of Engineering, James Cook University, QLD 4811, Australia

Received 19 February 2006; received in revised form 24 August 2006
Available online 2 November 2006

Abstract

An investigation of the natural convection boundary layer adjacent to an evenly heated semi-infinite plate with stratified ambient fluid is undertaken using scaling analysis and numerical simulation. The scaling analysis is shown to provide a complete description of the flow from start-up to full development, including the effect of the stratified ambient fluid. In particular it is shown that for the case with non-stratified ambient fluid the fully developed flow is y dependent over the entire plate, where y is the vertical coordinate, while for the case with stratified ambient fluid the fully developed flow is y dependent only in the region of the plate origin. A scaling is also obtained for the y dependent, y independent transition location. All the scalings are validated using a full numerical solution of the governing equations.

Keywords: Natural convection boundary layer; scaling

1. Introduction

Fluid adjacent to a heated vertical wall undergoes motion as the result of the transfer of heat from the wall into the fluid. The warmer fluid is, except in some special cases, less dense than its unheated surroundings, and rises relative to the ambient cooler fluid. The flow may be external, in which case the wall is located in a very large container of ambient fluid, or internal, in which case the wall is one of a closed container with other walls which may be heated, cooled or insulated. These natural convection flows are ubiquitous in nature and engineering, and form a class of flows of fundamental fluid mechanics interest.

Solutions for external flows with a doubly infinite wall, unsteady heating and a homogeneous ambient fluid have been available for many years (see for example [1–3]). However, in almost all actual applications, more realistic initial conditions are appropriate. In particular, a stratified ambient fluid is usual, and is in fact generally unavoidable. Solutions for the steady flow adjacent to a doubly infinite vertical plate with a stratified ambient were first obtained by [4]. Exact unsteady solutions for the case of an ambient stratification are evidently confined to those reported by [5,6], and more recently by [7,8]. In reality, vertical heated walls are not doubly infinite, and in every application will be of limited extent. The simplest model for this is a semi-infinite plate, with a leading edge. The response of this configuration to a variety of unsteady heating boundary conditions and a homogeneous ambient fluid has been extensively investigated experimentally and numerically, in the context of both internal cavity flows (for example [9–13] and others), and external flows (for example [3,14–20] and others). These investigations focussed on suddenly applied heating to the wall, with both isothermal and isoflux wall boundary conditions.

Thus there is a well developed understanding of the development of the thermal boundary layer adjacent to a semi-infinite plate for suddenly applied isothermal and isoflux heating, at least for those cases where the flow remains laminar. The understanding includes the transition of a boundary layer to steady-state by means of the leading

* Corresponding author. Tel.: +61 2 9351 2927; fax: +61 2 9351 7060.
E-mail address: armfield@aeromech.usyd.edu.au (S.W. Armfield).

0017-9310/$ - see front matter © 2006 Elsevier Ltd. All rights reserved.
doi:10.1016/j.ijheatmasstransfer.2006.08.020

Nomenclature

g	acceleration due to gravity
H	length scale
p	density normalised pressure
Pr	Prandtl number, ν/α
Ra	global Rayleigh number, $g\beta\Gamma_w H^4/\nu\alpha$
Ra_y	local Rayleigh number at height y, $g\beta\Gamma_w y^4/\nu\alpha$
Re	Reynolds number, $2\Gamma_w/Pr\Gamma_s$
t	time
t_s	time scale for the growth of thermal boundary layer
T	temperature
$\overline{T}$	perturbation temperature
T_w	plate temperature
T_{ws}	plate temperature scale at steady-state
$\overline{T}_y$	ambient temperature gradient
u	horizontal velocity
U	characteristic velocity, $\alpha Ra^{2/5}/H$
v	vertical velocity
v_s	vertical velocity scale at steady-state
x	horizontal coordinate
X	dimensionless horizontal limit of computational domain
y	vertical coordinate
y_{trans}	height of 2D to 1D transition
Y	dimensionless vertical limit of computational domain

Greek symbols

α	fluid thermal diffusivity
β	fluid thermal expansion coefficient
δ_T	thermal boundary layer thickness
δ_{Ts}	thermal boundary layer thickness scale at steady-state
ν	fluid kinematic viscosity
Γ_s	ambient temperature gradient
Γ_w	temperature gradient on plate
Δx	dimensionless minimum grid size in horizontal direction
Δy	dimensionless minimum grid size in vertical direction
Δt	dimensionless time step
ΔT	total temperature variation over boundary layer

Subscripts

t	first partial derivative with respect to t
x, y	first partial derivative with respect to x, y, respectively
xx, yy	second partial derivative with respect to x, y, respectively

edge effect and the stability properties of the subsequent steady boundary layer. However, none of these investigations into the unsteady behaviour of the semi-infinite plate dealt with the case in which the ambient fluid is stratified.

Scaling laws for the fully developed natural convection boundary layer adjacent to an evenly heated semi-infinite plate with an isoflux boundary condition have been developed, together with a set of ordinary differential equations derived from the governing equations using similarity transforms with a slow down-stream variation boundary layer assumption [21]. No such scales are currently available for the start up and transition to full development of the isoflux plate. Similarly an exact solution is available for the fully developed flow adjacent to an isoflux plate with stable linear background temperature gradient away from the plate origin [22], but no laws are currently available for the start up and transition phases of the flow, or for the behaviour of the flow in the region near the plate origin.

In this paper we develop scalings for the start-up, transition and full development of the natural convection boundary layer adjacent to an evenly heated isoflux semi-infinite plate, for both neutral and stable linear background stratification. The basic configuration is shown in Fig. 1. In particular we show using scaling that for the stratified case the fully developed flow far from the plat‘ leading edge is

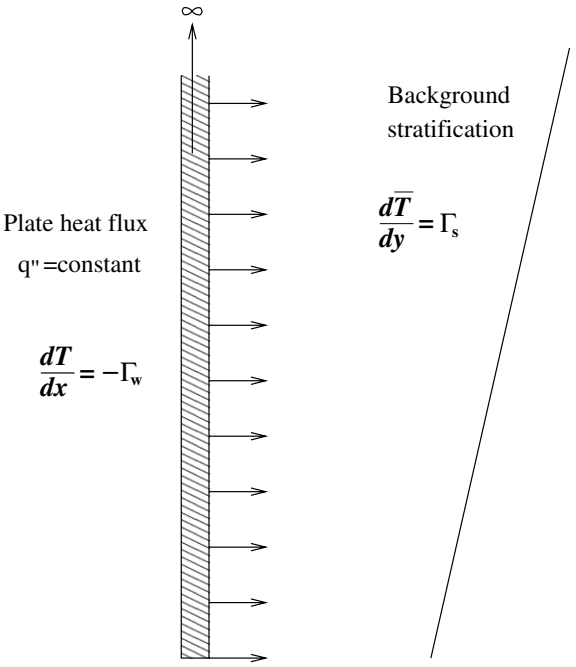

Fig. 1. Definition.

one dimensional, while that near the leading edge is two-dimensional. We obtain a scaling for the plate location at

which the one- to two-dimensional transition takes place. The scaling formulae are all validated using full numerical solutions of the governing Navier–Stokes equations for Prandtl number $Pr = 7.0$.

2. Scaling

The governing equations of motion are the Navier–Stokes equations expressed in two dimensional incompressible form with the Oberbeck–Boussinesq approximation for buoyancy, together with the temperature transport equation, as follows:

$$u_t + uu_x + vu_y = -p_x + v(u_{xx} + u_{yy}), \tag{1}$$

$$v_t + uv_x + vv_y = -p_y + v(v_{xx} + v_{yy}) + g\beta T, \tag{2}$$

$$u_x + v_y = 0, \tag{3}$$

$$T_t + uT_x + vT_y + v\Gamma_s = \alpha(T_{xx} + T_{yy}). \tag{4}$$

The temperature is represented as the sum of a background temperature $\overline{T}$ and a perturbation from the background temperature T. The temperature of the ambient fluid is assumed to be x independent and linear in y, with $\overline{T}_y = \Gamma_s$ either zero, corresponding to the non-stratified case, or positive and constant, corresponding to the stably stratified case. The plate lies at $x = 0$ with the origin at $y = 0$, with the plate boundary conditions

$$u = v = 0, \quad T_x = -\Gamma_w \quad \text{at } x = 0 \text{ for } y > 0, t \geqslant 0,$$

where the temperature gradient at the $x = 0$ boundary, $-\Gamma_w$, is a constant.

Scalings will be obtained for the vertical velocity v, the thermal boundary layer thickness δ_T, the start up time t_s, and the wall temperature T_w for both the stratified and non-stratified cases.

2.1. Non-stratified, $\Gamma_s = 0$

The scaling analysis follows that of [9], in which scales were derived for the start-up and full development of natural convection flow in a cavity with differentially heated isothermal walls. In this analysis it is assumed that the boundary layer thickness scale $\delta_T \ll y$ and the scaling is not expected to be applicable in the region very near to the plate origin.

The fluid is assumed to be initially quiescent with the wall heating started at time $t = 0$. Heat will then be conducted into the fluid adjacent to the wall creating a vertical layer of thickness $O(\delta_T)$, where from (4)

$$\delta_T \sim \alpha^{1/2} t^{1/2}. \tag{5}$$

Buoyancy forces accelerate the fluid in this layer. For $Pr > 1$ the buoyancy force in Eq. (2) will balance the viscous force, of order $O(v/\delta_T^2)$, in this region, giving

$$\frac{v}{\alpha t} \sim g\beta\Delta T,$$

where ΔT, the total temperature variation over the boundary layer, is of order $O(\Gamma_w \delta_T)$. Using (5) this may be written as

$$\Delta T \sim \Gamma_w \alpha^{1/2} t^{1/2}.$$

Combining these scalings then gives a relation for the boundary layer velocity scale during the start up phase as

$$v \sim \frac{g\beta\Gamma_w t^{3/2} v^{1/2}}{Pr^{3/2}}. \tag{6}$$

The boundary layer will continue to grow until the heat conducted into the fluid is balanced by that convected away by the vertical convection term in Eq. (4). The vertical convection term in Eq. (4) is of order $O(v\Delta T/y)$, while the conduction term is of order $O(\alpha\Delta T/\delta_T^2)$, balancing these terms will yield a scaling for the steady state velocity,

$$v_s \sim \frac{\alpha y}{\delta_T^2}. \tag{7}$$

A scaling for the time to steady-state is then obtained by combining relations (5)–(7) as follows:

$$\frac{g\beta\Gamma_w t^{3/2} v^{1/2}}{Pr^{3/2} y} \sim \frac{1}{t},$$

giving

$$t^{5/2} \sim \frac{Pr^{3/2} y}{g\beta\Gamma_w v^{1/2}},$$

so that the time scale for the growth of the thermal boundary layer is

$$t_s \sim \frac{y^2}{\alpha Ra_y^{2/5}}, \tag{8}$$

where $Ra_y = g\beta\Gamma_w y^4/v\alpha$ is the local Rayleigh number based on the plate location y.

An explicit form for the steady state velocity, v_s, is obtained by substituting relation (8) into (6),

$$v_s \sim \frac{g\beta\Gamma_w v^{1/2}}{Pr^{3/2}} \frac{y^{6/2}}{\alpha^{3/2} Ra_y^{6/10}} \rightarrow v_s \sim \frac{\alpha}{y} Ra_y^{2/5}. \tag{9}$$

The relation (8) may then be combined with (5) to obtain a scaling for the thermal boundary layer thickness at steady-state,

$$\delta_{Ts} \sim \frac{y}{Ra_y^{1/5}}. \tag{10}$$

The steady state temperature on the wall is then obtained from the thermal boundary layer thickness and the temperature gradient at the wall as

$$T_{ws} \sim \frac{\Gamma_w y}{Ra_y^{1/5}}. \tag{11}$$

The fully developed boundary layer with non-stratified ambient fluid then consists of a combined thermal/velocity boundary layer originating at the plate origin and increasing in thickness with vertical distance from the leading edge, as shown in Fig. 2.

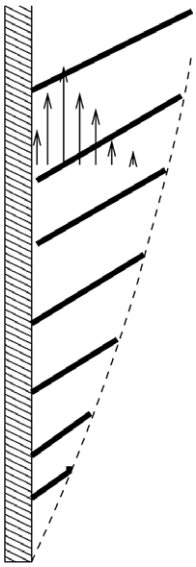

Fig. 2. Schematic of fully developed boundary layer for non-stratified ambient fluid.

An exact solution is available for the initial, unsteady phase of the flow development, presented in Goldstein and Briggs [3] for flow on an infinite plate. In this case the boundary layer continues to grow in time without bound. No exact solution is available for the fully developed flow on the semi-infinite plate, considered here, although an approximate solution may be obtained by solving a reduced set of simultaneous ordinary differential equations using a numerical method, as described in [21].

2.2. Stratified, $\Gamma_s > 0$

The scalings for the growth of the boundary layer when a background stratification is included are the same as those given above for no background stratification. The time to steady-state and the steady state behaviour will vary as a result of the extra vertical advection term in the temperature transport equation. Again steady-state will be achieved when the conduction of heat into the boundary layer is balanced by vertical convection in Eq. (4),

$$v(\Gamma_w\delta_T/y + \Gamma_s) \sim \frac{\alpha\Gamma_w\delta_T}{\delta_T^2}, \tag{12}$$

where $\Delta T \sim \Gamma_w\delta_T$. The first of these convection terms, $(v\Gamma_w\delta_T/y)$, is the same as that in the non-stratified case, while the second, $(v\Gamma_s)$, is that associated with the background stratification. If the first term is dominant then the steady state boundary layer will behave as for the non-stratified case and δ_T will be as given above in (10), in which case the first of the convection terms may be written as

$$\frac{\Gamma_w\delta_T}{y} \sim \frac{\Gamma_w}{y^{4/5}} \tag{13}$$

and this term is seen to reduce with increasing y. This term will therefore be dominant for small y and the boundary layer will behave as for the non-stratified case. For large y this term will be small and the term associated with the background stratification will be dominant. Thus for large y the appropriate scale balance is obtained from the second of the advection terms as

$$v\Gamma_s \sim \frac{\alpha\Gamma_w}{\delta_T}.$$

The velocity and boundary layer growth will be the same as for the non-stratified case above, $v \sim g\beta\Gamma_w t^{3/2}\nu^{1/2}/Pr^{3/2}$, $\delta_T \sim \alpha^{1/2}t^{1/2}$, which when substituted into the above expression gives

$$\frac{g\beta\Gamma_w t^{3/2}\nu^{1/2}}{Pr^{3/2}}\Gamma_s \sim \frac{\alpha^{1/2}\Gamma_w}{t^{1/2}}. \tag{14}$$

Extracting the time to steady-state for the stratified flow for large y then gives

$$t_s^2 \sim \frac{Pr}{\Gamma_s g\beta} \rightarrow t_s \sim \left(\frac{Pr}{\Gamma_s g\beta}\right)^{1/2}. \tag{15}$$

The scale for the thermal boundary layer thickness for the stratified flow at steady-state is then

$$\delta_{Ts} \sim \left(\frac{\alpha\nu}{\Gamma_s g\beta}\right)^{1/4} \tag{16}$$

and the velocity scale is

$$v_s \sim \Gamma_w\left(\frac{g\beta}{\nu}\right)^{1/4}\left(\frac{\alpha}{\Gamma_s}\right)^{3/4}. \tag{17}$$

The temperature on the wall at steady-state for the stratified flow is obtained as

$$T_{ws} \sim \Gamma_w\delta_T \sim \Gamma_w\left(\frac{\alpha\nu}{\Gamma_s g\beta}\right)^{1/4}. \tag{18}$$

The scaling analysis predicts that at steady-state for large y the thermal boundary layer thickness, velocity and wall temperature are independent of y. Therefore in the small y region near the plate origin the flow will behave as for no background stratification, reaching a y dependent steady-state. For large y the flow will develop to a steady state in which the thermal boundary layer thickness and velocity are y independent, and the full boundary temperature grows as the background stratification. This behaviour is shown in Fig. 3, where the quantity y_{trans} locates the point of transition from the small y two-dimensional flow to the large y one-dimensional flow. The large y flow has an exact solution that may be obtained by dropping all y dependent terms from the governing equations. This solution, given below in non-dimensional form in Eqs. (35) and (36), was obtained by Gill [4] for natural convection in a rectangular cavity and, in the context of mountain and valley winds, by Prandtl [23]. In a recent study by Shapiro and Fedorovich [7], in which an exact start-up

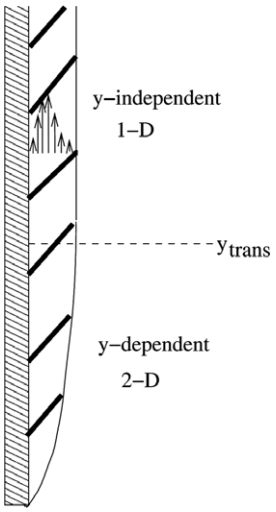

Fig. 3. Schematic of fully developed boundary layer for stratified ambient fluid.

solution for the $Pr = 1$ case on an infinite plate was derived, equivalent *y-independent* scalings to those presented here were used.

A scaling for y_{trans} is obtained as follows. It may be assumed that the point of transition will correspond to the location at which the two components of the vertical convection term in Eq. (4) are in balance, that is

$$\frac{\Gamma_w \delta_T}{y} \sim \Gamma_s.$$

Using the steady state boundary layer scale, δ_{Ts} then gives

$$y_{\text{trans}} \sim \frac{\Gamma_w}{\Gamma_s}\delta_{Ts} \sim \frac{\Gamma_w}{\Gamma_s}\left(\frac{\nu\alpha}{g\beta\Gamma_s}\right)^{1/4}. \tag{19}$$

This result may also be obtained by equating the scales for δ_{Ts} given by (10) and (16). However this δ_T scaling is only valid for $y_{\text{trans}} \gg \delta_{Ts}$, which from Eq. (19) requires that $\Gamma_s/\Gamma_w \ll 1$ (as $T_{ws} \sim \Gamma_w y/Ra^{1/5}$) . Otherwise the transition will occur in a region very close to the plate origin where the non-stratified δ_T scaling obtained above, which is based on the assumption that $\delta_T \ll y$, is not valid. In this region it may be assumed that the basic balance is between vertical and horizontal diffusion in the temperature equation

$$\alpha\frac{\Delta T}{\delta_T^2} \sim \alpha\frac{\Delta T}{y^2},$$

giving the relation $\delta_T \sim y$, which will then provide the scaling for the transition point

$$y_{\text{trans}} \sim \delta_T.$$

With δ_T obtained from the steady state stratified scaling this gives

$$y_{\text{trans}} \sim \left(\frac{\nu\alpha}{g\beta\Gamma_s}\right)^{1/4}, \tag{20}$$

for large Γ_s/Γ_w.

The behaviour of the boundary layer with stratified ambient fluid in the small y region is therefore determined by the ratio of the stratification to the horizontal temperature gradient on the boundary, Γ_s/Γ_w. For all Γ_s/Γ_w a diffusive region will exist for very small y, for large Γ_s/Γ_w the flow will transit directly to the one-dimensional boundary layer with increasing y, while for small Γ_s/Γ_w an intermediate y region will exist in which the flow obeys the non-stratified scaling relations.

3. Numerical results

3.1. Non-stratified, $\Gamma_s = 0$

The governing equations are recast in non-dimensional form using the characteristic velocity and time scales given above. This also requires a characteristic length scale, however in the semi-infinite plate flow considered here there is no natural fixed geometric length scale, the only natural scales are the distance from the plate origin and the boundary layer thickness, which are both variable. In this case it is common to choose an arbitrary characteristic length, here denoted H, to allow the equations to be non-dimensionalised [15]. For the non-stratified flow the characteristic velocity is, from (9), $U = \frac{\alpha}{H}Ra^{2/5}$, the characteristic time is, from (8), $t = H^2/(\alpha Ra^{2/5})$ and the characteristic temperature is $T = \Gamma_w H$ (the full form of (11) is not used for the temperature scaling as that would require the inclusion of the Rayleigh number in the boundary conditions). The non-dimensional equations are then

$$u_t + uu_x + vu_y = -p_x + \frac{Pr}{Ra^{2/5}}(u_{xx} + u_{yy}), \tag{21}$$

$$v_t + uv_x + vv_y = -p_y + \frac{Pr}{Ra^{2/5}}(v_{xx} + v_{yy}) + PrRa^{1/5}T, \tag{22}$$

$$u_x + v_y = 0, \tag{23}$$

$$T_t + uT_x + vT_y + v\overline{T_y} = \frac{1}{Ra^{2/5}}(T_{xx} + T_{yy}). \tag{24}$$

All quantities, u, v, p, T, t, x, y are now non-dimensional. Some insight into the behaviour of the solution may also be obtained by inspecting the non-dimensional equations. Increasing the Rayleigh number is seen to correspond to a reduction in viscous and diffusive effects, and would therefore be expected to be associated with the onset of instability and turbulence. Increasing the Prandtl number will proportionally reduce the diffusive effects with respect to the viscous effects, reducing the stabilising effect of the diffusive terms.

The governing equations are discretised on a non-staggered mesh using finite volumes, with standard second-order central difference schemes used for the viscous, pressure gradient and divergence terms. The QUICK third-order upwind scheme [24], which has been widely used for buoyancy-affected flows [25–32], is used for the advective terms. The second-order Adams–Bashforth scheme and Crank–Nicolson scheme are used for the time integration of the advective terms and the diffusive terms, respectively. To enforce continuity, the pressure correction

approach is used to construct a Poisson's equation which is solved using the preconditioned GMRES method. Detailed descriptions of these schemes are given in [33–35] and the code has been widely used for the simulation of a range of buoyancy dominated flows (see, e.g., [36–42]).

3.1.1. Domain and boundary conditions

The semi-infinite vertical plate in an infinite domain is modelled by solving the non-dimensional governing equations in the domain $-0.2 \leqslant y \leqslant 1.5,\ 0 \leqslant x \leqslant 0.5,\ t \geqslant 0$, with the boundary conditions

$$u = v = 0, \quad T_x = -1 \quad \text{at } x = 0 \text{ for } y > 0,$$
$$u = v = 0, \quad T_x = 0 \quad \text{at } x = 0 \text{ for } y < 0,$$
$$u_x = T_x = v = 0 \quad \text{for } x = 0.5,$$
$$u_{yy} = v_{yy} = T_{yy} = 0 \quad \text{for } y = 1.5,$$
$$u = v = T_y = 0 \quad \text{for } y = -0.2.$$

At time $t < 0$ the fluid is quiescent and isothermal with $T = 0$. At time $t = 0$ the above boundary conditions are applied and the flow is allowed to develop.

The domain is discretised with a non-uniform rectangular grid with $\Delta x = 2.0 \times 10^{-4}$ at the wall, expanding at a maximum rate of 5% away from the wall and $\Delta y = 5.0 \times 10^{-4}$ at $y = 0$, expanding at a maximum rate of 5% away from $y = 0$. This gives a grid of 89×194 nodes in the x and y directions respectively. A time-step of $\Delta t = 1.5 \times 10^{-4}$ has been used. An extensive mesh and time-step dependency analysis has been carried out to ensure that the solution is accurate for these values. Additionally tests have been carried out to ensure the finite domain size is not affecting the accuracy of the solution at the locations shown below.

3.1.2. Non-dimensional scales

The scaling relations are also converted to non-dimensional form using the characteristic velocity, length and temperature scales given above. During the start-up phase of the flow the non-dimensional velocity and time scales are obtained in non-dimensional form as

$$v \sim t^{3/2}, \tag{25}$$
$$\delta_T \sim \frac{t^{1/2}}{Ra^{1/5}}. \tag{26}$$

Time to steady-state, boundary layer thickness, velocity and wall temperature at steady-state, are obtained as

$$t_s \sim y^{2/5}, \tag{27}$$
$$\delta_{Ts} \sim \frac{y^{1/5}}{Ra^{1/5}}, \tag{28}$$
$$v_s \sim y^{3/5}, \tag{29}$$
$$T_{ws} \sim \frac{y^{1/5}}{Ra^{1/5}}. \tag{30}$$

3.1.3. Results

Fig. 4 contains fully developed stream function and temperature contours for the case with a non-stratified ambient fluid, $Ra = 3 \times 10^8$ and $Pr = 7.0$. The stream function contours show the basic structure of the flow, with the boundary layer formed adjacent to the heated part of the $x = 0$ boundary, $y \geqslant 0$, entraining fluid through the far-field open boundary and discharging it downstream. The temperature contours clearly show the heated region of the $x = 0$ boundary, corresponding to the heated plate, and show the increase in width and intensity with increasing y.

Fig. 5 contains the temperature time series obtained at four heights on the heated plate. Fig. 5(a) contains the raw data showing the basic development of the flow, with all the time series overlaying each other for early time showing the one-dimensional nature of the early time flow. With increasing time the lower y value time series diverge from the higher y values, showing the transition to two-dimensional flow at each height. After divergence the temperature continues to develop at each height, passing through a small overshoot and ultimately reaching a steady state. Fig. 5(b) shows the same time series results, but with both the temperature scaled by $y^{1/5}$ and time scaled by $y^{2/5}$, the steady state scaling for the wall temperature T_{ws}, and the scaling for time to steady-state, t_s, respectively. The scalings clearly collapse the solutions onto a single curve validating the relations. In Fig. 5(c) the time is further scaled by taking its square root, reflecting the start-up behaviour given in (26), with the resulting linear relation between $T/y^{1/5}$ and $(t/y^{2/5})^{1/2}$ in the region $(t/y^{2/5})^{1/2} < 1.5$ validating this relation.

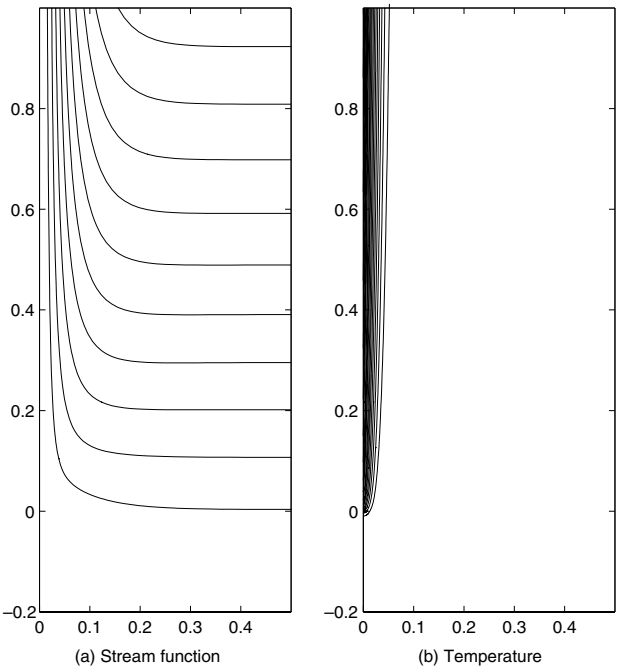

Fig. 4. Stream function and temperature contours for the fully developed non-stratified flow.

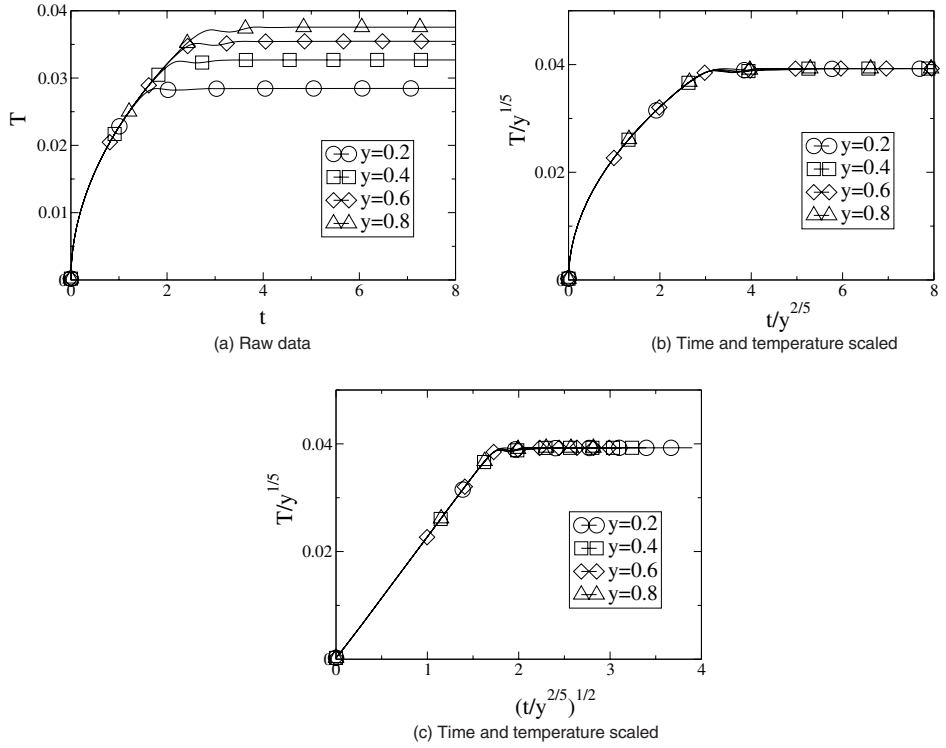

Fig. 5. Temperature time series in raw and scaled form for the non-stratified flow.

Fig. 6 contains horizontal profiles of the vertical velocity at four heights at steady-state, with the raw data shown in Fig. 6(a). The profiles show the typical structure of the natural convection boundary layer, with a large shear layer adjacent to the heated plate and a lower shear layer reaching into the far field, with the velocity there reducing to zero. The scalings obtained above show that the velocity will depend on $y^{3/5}$, and the boundary layer width will depend on $y^{1/5}$. The vertical velocity profiles with these scalings are shown in Fig. 6(b), where it is seen that the solutions are collapsed onto a single curve, validating these relations.

Fig. 7 contains the temperature profiles at a range of heights, with the raw data shown in Fig. 7(a). The temperature on the plate and the boundary layer width are seen to increase with height. The scaling shows that the plate temperature will depend on $y^{1/5}$, and the boundary layer width will also depend on $y^{1/5}$. The scaled results are presented in Fig. 7(b) showing that the scalings collapse all the solutions onto a single curve, validating these relations.

It is noted that while the velocity and temperature boundary layers obey the same scaling relation for width, that is $\delta_T \sim y^{1/5}$, the velocity boundary layer is considerably thicker than the thermal boundary layer. The velocity boundary layer will grow at order $O(v^{1/2}t^{1/2})$ and it is therefore expected that the velocity boundary layer thickness $\delta_v \sim Pr^{1/2}\delta_T$, making the velocity boundary layer approximately 2.5 times thicker than the thermal boundary layer for Prandtl number $Pr = 7$, as observed here.

3.2. Stratified, $\Gamma_s > 0$

The scaling analysis given above indicates the stratified flow has two distinct regions, a small y region in which

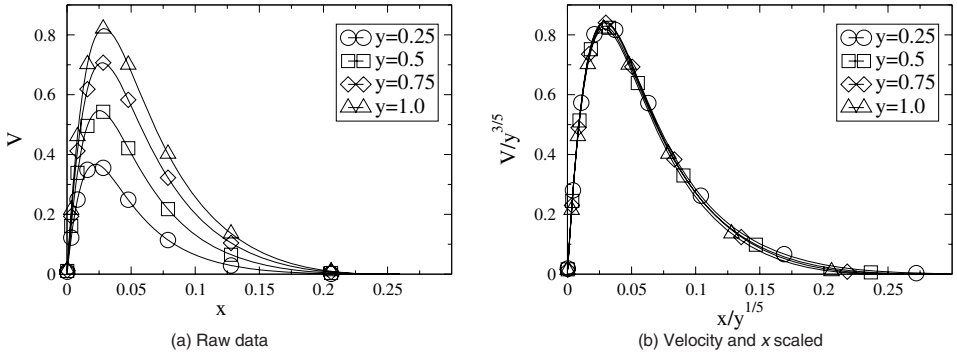

Fig. 6. Vertical velocity profiles in raw and scaled form for the fully developed non-stratified flow.

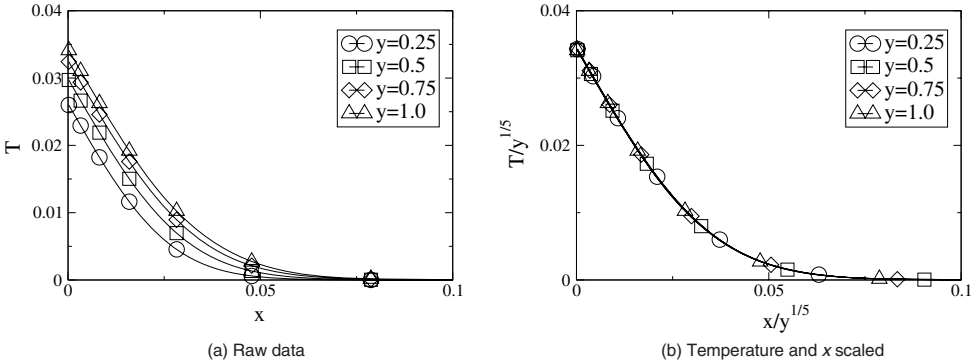

Fig. 7. Temperature profiles in raw and scaled form for the fully developed non-stratified flow.

the fully developed flow is y dependent, and a large y region in which the fully developed flow is independent of y. This behaviour is associated with different scaling relations. In this section the effect of the stratification on the flow will be demonstrated, and as such it is appropriate to recast the governing equations in non-dimensional form using the scalings associated with the large y region. The characteristic velocity, length, time and temperature scales are then obtained from the scalings for the steady state velocity, boundary layer thickness and wall temperature in the large y region, as

$$U = \sqrt{2}\Gamma_w \left(\frac{g\beta}{\nu}\right)^{1/4} \left(\frac{\alpha}{\Gamma_s}\right)^{3/4},$$

$$\delta = \sqrt{2}\left(\frac{\alpha\nu}{g\beta\Gamma_s}\right)^{1/4},$$

$$t = \frac{1}{\Gamma_w}\left(\frac{\nu\Gamma_s}{g\alpha\beta}\right)^{1/2},$$

$$\Delta T = \Gamma_w \delta.$$

This gives the non-dimensional equations

$$u_t + uu_x + vu_y = -p_x + \frac{1}{Re}(u_{xx} + u_{yy}), \tag{31}$$

$$v_t + uv_x + vv_y = -p_y + \frac{1}{Re}(v_{xx} + v_{yy}) + \frac{2}{Re}T, \tag{32}$$

$$u_x + v_y = 0, \tag{33}$$

$$T_t + uT_x + vT_y + v\frac{2}{RePr} = \frac{1}{RePr}(T_{xx} + T_{yy}). \tag{34}$$

where the Reynolds number $Re = \frac{\Gamma_w 2}{\Gamma_s Pr}$. The $\sqrt{2}$ in the velocity and length scalings given above has been included to normalise the scaled exact solution for $T(x)$, given in Eq. (36) below, such that $T(0) = 1.0$. Again all quantities u, v, p, T, t, x, y are now non-dimensional and the numerical scheme is as described above. Inspection of the scaled non-dimensional equations shows that an increase in Re will lead to a reduction in viscous and diffusive effects and would be associated with instability, as well as reducing the coupling between the dynamics and the thermo-dynamics.

3.2.1. Domain and boundary conditions

The governing equations are solved in the domain $-Y/5 \leqslant y \leqslant Y$, $0 \leqslant x \leqslant X$, $t \geqslant 0$, with the boundary conditions

$$u = v = 0, \quad T_x = -1 \quad \text{at } x = 0 \text{ for } y > 0,$$
$$u = v = 0, \quad T_x = 0 \quad \text{at } x = 0 \text{ for } y < 0,$$
$$u_x = T_x = v = 0 \quad \text{for } x = X,$$
$$u_{yy} = v_{yy} = T_{yy} = 0 \quad \text{for } y = Y,$$
$$u = v = T_y = 0 \quad \text{for } y = -Y/5,$$

where Y is chosen large enough at each Re to ensure that $Y \gg y_{\text{trans}}$ for that flow. The limit on X was then largely determined by numerical stability constraints, with X being increased with Y, even though the boundary layer width δ_{Ts} is constant in the scaled variables. For example at $Re = 0.14$, $Y = 200$, $X = 15$, while at $Re = 140$, $Y = 2000$, $X = 40$. An appropriate grid size and time step was also

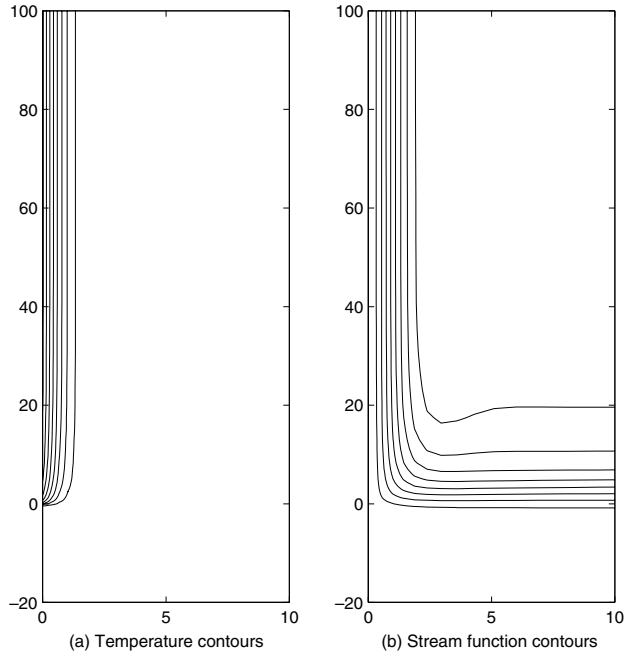

Fig. 8. Stream function and temperature contours for the fully developed stratified background flow.

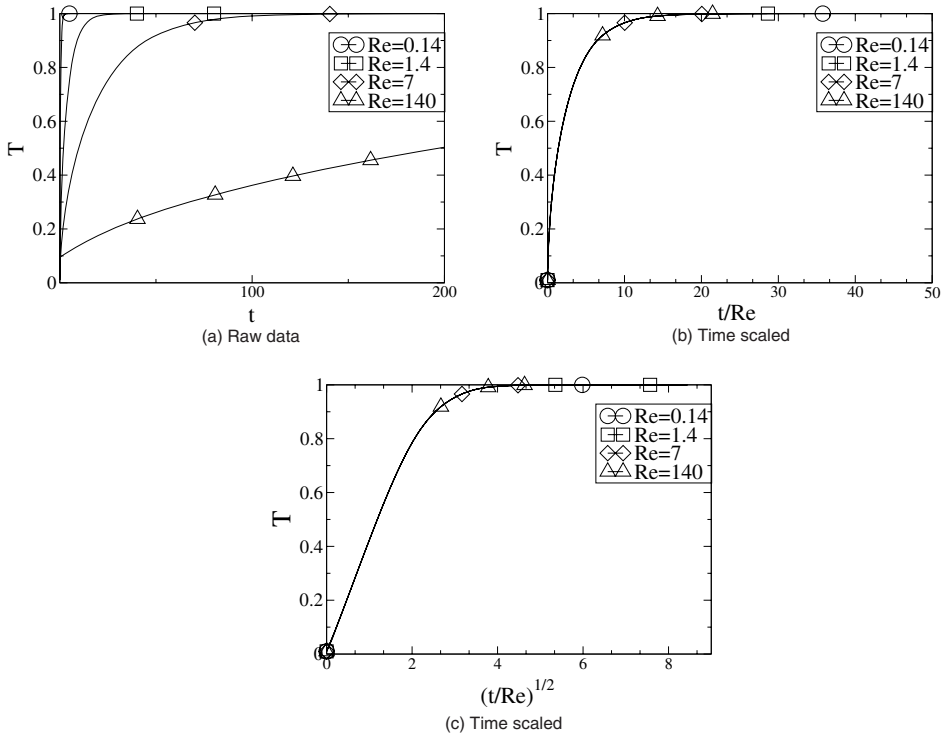

Fig. 9. Temperature time series for the stratified background flow.

determined for each Re, with $\Delta x = 0.01$ for all cases, Δy varying from 0.1 for $Re = 0.014$ to 2 for $Re = 140$ and Δt varying from 2×10^{-5} for $Re = 0.014$ to 2×10^{-3} for $Re = 140$, with the grid stretching again limited to a maximum of 5%.

3.2.2. Non-dimensional scales

The scaling for the stratified flow presented above suggests that away from the plate origin for $y > y_{\text{trans}}$, the temperature and velocity fields will be independent of y. Applying this assumption to the scaled equations for the stratified flow, given above, allows all y derivative terms to be dropped and an analytic solution to be obtained of the form [4,23]

$$v(x) = \mathrm{e}^{-x} \sin x, \tag{35}$$

$$T(x) = \mathrm{e}^{-x} \cos x. \tag{36}$$

Non-dimensional time to steady-state in the $y > y_{\text{trans}}$ region will be

$$t_{\text{s}} \sim RePr. \tag{37}$$

In the scaling section two relations were obtained for y_{trans}, (19) for small $\Gamma_{\text{s}}/\Gamma_{\text{w}}$ and (20) for large $\Gamma_{\text{s}}/\Gamma_{\text{w}}$. From the definition of the Reynolds number given above, small $\Gamma_{\text{s}}/\Gamma_{\text{w}}$ corresponds to large Re, and vice-versa. Therefore the two scalings for y_{trans} in non-dimensional form will be; for large Re,

$$y_{\text{trans}} \sim Re, \tag{38}$$

and for small Re,

$$y_{\text{trans}} \sim \mathrm{O}(1). \tag{39}$$

3.2.3. Results

Fig. 8 contains the stream function and temperature contours for the fully developed flow with stratified ambient fluid for $Re = 7$ and $Pr = 7$. In this case the horizontal direction has been stretched to more clearly show the structure of boundary layer, which is otherwise too narrow to allow the features to be readily discerned. The flow has a region of y variation near to the plate origin, while away from this region the flow is one-dimensional with no y variation, as predicted by the scaling analysis.

Fig. 9 contains the temperature time series obtained on the plate for four Reynolds numbers. For each Reynolds number the height chosen is such that the flow at the large

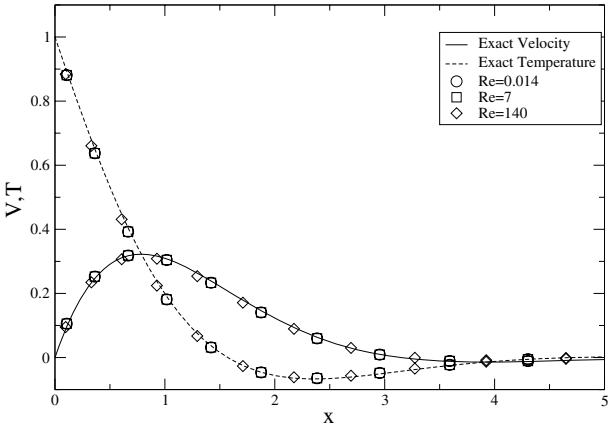

Fig. 10. Numerical vertical velocity and temperature profiles compared to exact solution for stratified background flow.

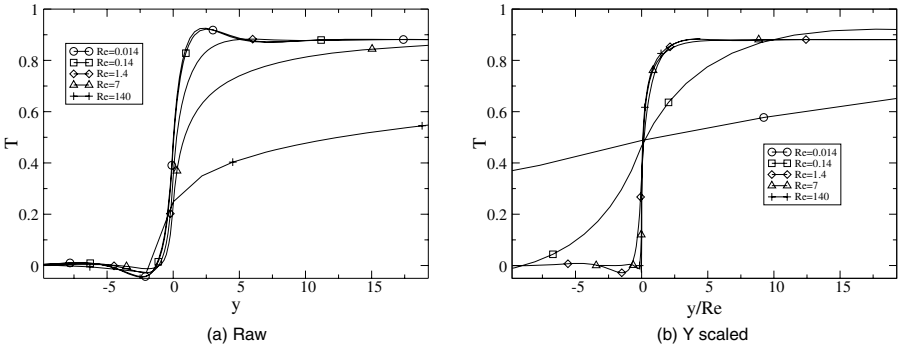

Fig. 11. Vertical temperature variation with y at $x = 0$ for the fully developed stratified background flow.

y boundary is in the one-dimensional region at steady-state, and the locations of the time-series have been chosen to ensure that they are in the one-dimensional region. Fig. 9(a) contains the raw results, where the large variation in development time is seen. The data with time scaled by Re are shown in Fig. 9(b) where it is seen that all the solutions are collapsed onto a single curve, validating the scaling relation for time to full development in the flow with stratified ambient fluid. The scaled time has been further scaled by taking its square root, shown in Fig. 9(c). The start-up scales for the stratified flow are expected to be the same as those for the non-stratified flow, which has been shown to have a square-root relation with time during the start-up phase. In Fig. 9(c) a linear relation is seen to exist between T and $(t/Re)^{1/2}$ for $(t/Re)^{1/2} < 1.5$ indicating during this phase of the start-up the temperature is behaving as for the non-stratified flow. During the later stages of start-up, as the flow transitions to steady-state, the relation is seen to diverge from linear, indicating that the stratified flow is diverging from the non-stratified behaviour.

Fig. 10 contains horizontal profiles of the vertical-velocity and temperature obtained at three Reynolds numbers in the upper, y independent, region of the flow, together with the exact y independent solution given above in Eqs. (35) and (36). As can be seen the numerical solutions exactly match the analytic solutions, confirming the accuracy of the numerical result and further validating the scaling result showing that the large y boundary layer is y independent at full development.

Fig. 11 contains the vertical variation of the temperature at full development on the plate, at $x = 0.0$, for five Reynolds numbers. Fig. 11(a) shows the raw data where it is seen that the extent of the y dependent regions increase with Reynolds number. For the highest Reynolds numbers shown the y extent of the graph is not sufficient to show the transition to y independence, however all results do show a transition to y independence, with y_{trans} at approximately $y = 1400$ for the $Re = 140$ result. In non-dimensional form the scaling for y_{trans} for strong stratification is $y_{\text{trans}} \sim \text{O}(1)$, while for weak stratification, $y_{\text{trans}} \sim Re$. Strong stratification corresponds to small Re, and in Fig. 11(a) it is seen that the temperature profiles for $Re < 1$ lie approximately on top of each other indicating that y_{trans} is then independent of Re as predicted by the scaling. The same results are shown in Fig. 11(b), but with y divided by Re. In this case the $Re > 1$ results lie approximately on top of each other confirming the scaling prediction for weak stratification. It is observed that for $Re < 1$, $y_{\text{trans}} \simeq 10$ and for $Re > 1$, $y_{\text{trans}} \simeq 10Re$.

4. Conclusions

Scaling relations for the start-up, transition and full development of the natural convection boundary layer adjacent to an evenly heated vertical semi-infinite plate with isoflux boundary condition have been obtained. The scalings describe the rate of growth of the boundary layer velocity, temperature and thermal boundary layer width, as well as the transition time and fully developed values, for both neutral and stable linearly stratified ambient fluids. In particular the scaling results indicate that at full development the stratified case will have a region of two-dimensional flow near to the plate origin, while the remainder of the flow, far from the plate origin, will be one-dimensional.

The scaling results provided appropriate velocity and time scales for the non-stratified case. The governing equations were non-dimensionalised using these scales together with an arbitrary length scale, showing that the control parameters for this flow are a Rayleigh number, based on the length scale H, and the Prandtl number Pr. Numerical solutions to the non-dimensionalised equations were used to validate the scaling relations.

The scaling results showed that the appropriate length scale for the stratified case, far from the plate origin, is the boundary layer thickness. Using this and the boundary layer velocity to non-dimensionalise the governing equations shows that the control parameters are the Prandtl number and the temperature gradient ratio Γ_s/Γ_w. The equations were written in terms of a Reynolds number that is inversely proportional to the temperature gradient ratio. It appears that there is no similarity transformation relating the fully developed stratified flow far from the plate origin to the fully developed non-stratified flow, as allowing $\Gamma_s \to 0$ gives $Re \to \infty$. The assumption that the fully developed stratified flow is one-dimensional far from the plate

origin allows an analytic solution to be obtained that is independent of the control parameters. The scaling for transition from the near plate origin two-dimensional flow to the one-dimensional flow has two forms; for large *Re* it varies with the Reynolds number, while for small *Re* it is O(1). Numerical solutions confirmed that the analytic solution is correct for the one-dimensional region of the fully developed flow, and that the start-up and transition behaviour is correctly predicted by the time scaling. The scaling for the two- to one-dimensional transition location was also shown to be correctly represented by the scaling relation.

Acknowledgement

The authors wish to acknowledge the support of the Australian Research Council.

References

[1] C.R. Illingworth, Unsteady laminar flow of gas near an infinite flat plate, Proc. Cambridge Philos. Soc. 46 (1950) 603–613.
[2] J.A. Schetz, R. Eichhorn, Unsteady natural convection in the vicinity of a doubly infinite vertical plate, Trans. ASME J. Heat Transfer 84 (1962) 334–338.
[3] R.J. Goldstein, D.G. Briggs, Transient free convection about vertical plates and circular cylinders, Trans. ASME J. Heat Transfer 86 (1964) 490–500.
[4] A.E. Gill, The boundary layer regime for convection in a rectangular cavity, J. Fluid Mech. 26 (1966) 515–536.
[5] J.S. Park, J. Hyun, Transient behavior of vertical buoyancy layer in a stratified fluid, Int. J. Heat Mass Transfer 41 (1998) 4393–4397.
[6] J.S. Park, Transient buoyant flows of a stratified fluid in a vertical channel, KSME Int. J. 15 (2001) 656–664.
[7] A. Shapiro, E. Fedorovich, Unsteady convectively driven flow along a vertical plate immersed in a stably stratified fluid, J. Fluid Mech. 498 (2004) 333–352.
[8] A. Shapiro, E. Fedorovich, Prandtl number dependence of unsteady natural convection along a vertical plate in a stably stratified fluid, Int. J. Heat Mass Transfer 47 (2004) 4911–4927.
[9] J.C. Patterson, J. Imberger, Unsteady natural convection in a rectangular cavity, J. Fluid Mech. 100 (1980) 65–86.
[10] J.C. Patterson, S.W. Armfield, Transient features of natural convection in a cavity, J. Fluid Mech. 219 (1990) 469–497.
[11] S.W. Armfield, J.C. Patterson, Wave properties of natural-convection boundary layers, J. Fluid Mech. 239 (1992) 195–211.
[12] A.M.H. Brooker, J.C. Patterson, T. Graham, W. Schopf, Convective instability in a time-dependent buoyancy driven boundary layer, Int. J. Heat Mass Transfer 43 (2000) 297–310.
[13] J.C. Patterson, T. Graham, W. Schopf, S.W. Armfield, Boundary layer development on a semi-infinite suddenly heated vertical plate, J. Fluid Mech. 453 (2002) 39–55.
[14] R. Seigel, Transient free convection from a vertical flat plate, Trans. ASME J. Heat Transfer 80 (1958) 347–359.
[15] S.N. Brown, N. Riley, Flow past a suddenly heated vertical plate, J. Fluid Mech. 59 (1973) 225–237.
[16] D.B. Ingham, Flow past a suddenly heated vertical plate, Proc. Roy. Soc. London A 402 (1985) 109–134.
[17] R.L. Mahajan, B. Gebhart, Higher order approximations to the natural convection flow over a uniform flux vertical surface, Int. J. Heat Mass Transfer 21 (1978) 549–556.
[18] Y. Joshi, B. Gebhart, Transition of transient vertical natural-convection flows in water, J. Fluid Mech. 179 (1987) 407–438.
[19] P.G. Daniels, J.C. Patterson, On the long-wave instability of natural-convection boundary layers, J. Fluid Mech. 335 (1997) 57–73.
[20] P.G. Daniels, J.C. Patterson, On the short-wave instability of natural convection boundary layers, Proc. Roy. Soc. London A 457 (2001) 519–538.
[21] E.M. Sparrow, J.L. Gregg, Laminar free convection from a vertical plate with uniform surface heat flux, Trans. ASME 78 (1956) 435–440.
[22] G.D. McBain, S.W. Armfield, Linear stability of natural convection on an evenly heated vertical wall, in: M. Behnia, W. Lin, G.D. McBain (Eds.), Proceedings of the 15th Australasian Fluid Mechanics Conference, Sydney, Australia, December 13–17, 2004, Paper AFMC00196.
[23] L. Prandtl, Essentials of Fluid Mechanics, Blackie, London, 1952.
[24] B.P. Leonard, A stable and accurate convective modelling procedure based on quadratic upstream interpolation, Comput. Methods Appl. Mech. Eng. 19 (1979) 59–98.
[25] S. Thakur, W. Shyy, Some implementational issues of convection schemes for finite-volume formulations, Numer. Heat Transfer B: Fundam. 24 (1993) 31–55.
[26] P. Johansson, L. Davidson, Modified collocated SIMPLEC algorithm applied to buoyancy-affected turbulent-flow using a multigrid solution procedure, Numer. Heat Transfer B: Fundam. 28 (1995) 39–57.
[27] M.M. Rahman, A. Miettinen, T. Siikonen, Modified SIMPLE formulation on a collocated grid with an assessment of the simplified QUICK scheme, Numer. Heat Transfer B: Fundam. 30 (1996) 291–314.
[28] M.M. Rahman, T. Siikonen, A. Miettinen, A pressure-correction method for solving fluid flow problems on a collocated grid, Numer. Heat Transfer B: Fundam. 32 (1997) 63–84.
[29] R.G. Rajagopalan, C.J. Yu, Use of Lagrange interpolation in modeling convective kinematics, Numer. Heat Transfer B: Fundam. 36 (1999) 233–240.
[30] Z.H. Yan, A numerical study of effect of initial condition on large eddy simulation of thermal plume, Numer. Heat Transfer B: Fundam. 43 (2003) 167–178.
[31] A. Sergent, P. Joubert, P. Le Quéré, Development of a local subgrid diffusivity model for large-eddy simulation of buoyancy-driven flows: application to a square differentially heated cavity, Numer. Heat Transfer A: Appl. 44 (2003) 789–810.
[32] M.A. Randriazanamparany, A. Skouta, M. Daguenet, Numerical study of the transition toward chaos of two-dimensional natural convection within a square cavity, Numer. Heat Transfer A: Appl. 48 (2005) 127–147.
[33] S.W. Armfield, Finite difference solutions of the Navier–Stokes equations on staggered and non-staggered grids, Comput. Fluids 20 (1991) 1–17.
[34] S.W. Armfield, Ellipticity, accuracy and convergence of the discrete Navier–Stokes equations, J. Comput. Phys. 114 (1994) 176–184.
[35] S.W. Armfield, R. Street, Fractional step methods for the Navier–Stokes equations on non-staggered grids, ANZIAM J. 42 (2000) C134–C156.
[36] S.W. Armfield, J.C. Patterson, Direct simulation of wave interactions in unsteady natural convection in a cavity, Int. J. Heat Mass Transfer 34 (1991) 929–940.
[37] S.W. Armfield, W. Debler, Purging of density stabilized basins, Int. J. Heat Mass Transfer 36 (1993) 519–530.
[38] W. Lin, S.W. Armfield, Direct simulation of natural convection cooling in a vertical circular cylinder, Int. J. Heat Mass Transfer 42 (1999) 4117–4130.
[39] W. Lin, S.W. Armfield, Direct simulation of weak axisymmetric fountains in a homogeneous fluid, J. Fluid Mech. 403 (2000) 67–88.
[40] W. Lin, S.W. Armfield, Very weak fountains in a homogeneous fluid, Numer. Heat Transfer A: Appl. 38 (2000) 377–396.
[41] W. Lin, S.W. Armfield, Long-term behavior of cooling fluid in a rectangular container, Phys. Rev. E 69 (2004) 056315.
[42] W. Lin, S.W. Armfield, Long-term behavior of cooling fluid in a vertical cylinder, Int. J. Heat Mass Transfer 48 (2005) 53–66.